

This is the accepted version of the article:

Cordero-Edwards K., Kianirad H., Canalias C., Sort J., Catalan G.. Flexoelectric Fracture-Ratchet Effect in Ferroelectrics. Physical Review Letters, (2019). 122. 135502: - . 10.1103/PhysRevLett.122.135502.

Available at:

<https://dx.doi.org/10.1103/PhysRevLett.122.135502>

Flexoelectric fracture-ratchet effect in ferroelectrics

Kumara Cordero-Edwards^{1*}, Hoda Kianirad², Carlota Canalias², Jordi Sort^{3, 4}, and Gustau Catalan^{1, 4*}

¹ Catalan Institute of Nanoscience and Nanotechnology (ICN2), CSIC and BIST, Campus UAB, Bellaterra, Barcelona 08193, Catalonia.

² Department of Applied Physics, KTH-Royal Institute of Technology, Roslagstullsbacken 21, 10691, Stockholm, Sweden

³ Departament de Física, Universitat Autònoma de Barcelona (UAB), Edifici Cc, E-08193 Bellaterra, Barcelona, Catalonia

⁴ Institut Catalana de Recerca i Estudis Avançats (ICREA), Pg. Lluís Companys 23, E-08010 Barcelona, Catalonia.

* Corresponding author:

Email: rohini.corderoedwards@unige.ch Tel: + 41 022 379 30 34

Email: gustau.catalan@icn2.cat Tel: + 34 93 737 3618

 Now at University of Geneva

Abstract

The propagation front of a crack generates large strain gradients and it is therefore a strong source of gradient-induced polarization (flexoelectricity). Herein, we demonstrate that, in piezoelectric materials, a consequence of flexoelectricity is that crack propagation is helped or hindered depending on whether it is parallel or antiparallel to the piezoelectric polar axis. The discovery of crack propagation asymmetry implies that fracture physics cannot be assumed to be symmetric in polar materials, and it demonstrates that flexoelectricity must be incorporated in any realistic model. The results also have potential practical repercussions for electromechanical fatigue of ferroelectric films and piezoelectric transducers, and provide a new degree of freedom for crack-based nanopatterning.

Crack propagation causes materials to break, and forms basis of fracture physics a vital element of materials science and engineering as it determines the mechanical resilience of devices.^[1-2] Fascinatingly, controlled cracking has also been proposed as a mechanism for device nano-patterning,^[3] turning the harnessing of crack propagation into a constructive pursuit. In the specific case of piezoelectric and ferroelectric materials, fracture physics is additionally important because voltage-induced strains cause the appearance and propagation of microcracks that result in material fatigue and ultimate failure of piezoelectric transducers.^[4-5] The fracture physics of piezoelectrics is therefore a fundamental problem with important practical ramifications. Here we show that crack-generated flexoelectricity causes in ferroelectrics an original valve-like or “crack filter” behavior, whereby crack propagation is facilitated or impaired depending on the sign of the ferroelectric polarization. In other words, the toughness of ferroelectrics is, like their polarization, switchable.

Flexoelectricity^[6-8] has disruptive consequences for the physics of materials, enabling new behaviors^[9-12] For example, it has recently been predicted^[12] and demonstrated^[13] that ferroelectrics can have an asymmetric mechanical response to inhomogeneous deformations. Because fracture fronts concentrate the biggest local deformations that a solid can withstand, flexoelectricity is also expected to affect fracture behavior. For example, the flexoelectric fields generated by cracks are strong enough to be able to trigger the self-repair process in bone fractures.^[14] The present work demonstrates a new fracture phenomenon due to the interplay between flexoelectricity and ferroelectricity: that crack propagation in ferroelectrics is asymmetric and switchable, so that cracks propagating parallel to the ferroelectric polarization become longer than those travelling against it.

In the present experiment, Vickers Indentation Tests were performed on a Rb-doped KTiOPO₄ (RKTP) single crystal with the polarization in-plane. We chose this ferroelectric because it is uniaxial, and thus ferroelastic effects can be excluded. RKTP is also a

technologically relevant material, commonly used as a frequency conversion device in nonlinear optics.^[15-16] For such applications, a bulk periodic domain pattern with alternating domain orientations (periodic poling) is created in the crystal. The procedure for this is well-established,^[15] which facilitates the in-plane poling the crystal. Poling of antiparallel domains on the same crystal was used, in order to ensure that geometrical effects such as a slight tilt or miscut of the crystal surface did not affect the results. By poling two domains of antiparallel orientation, indents could be performed on domains of opposite polarity on the same crystal surface and in the same experiment, as sketched in Fig. 1(a). That way, the effect of alternating polarity was tested without affectation from any other spurious effect such as variations in sample geometry or chemistry.

Mechanical tests were conducted by applying sets of 200mN and 300mN loads, with the orientation of the indenter being such that two of its four corners were parallel to the polar axis and the other two perpendicular. In order to control for statistical fluctuations in fracture toughness, 30 indents for each force (15 for each domain polarity) were performed, with each indent generating four cracks along the parallel, antiparallel and perpendicular directions. In total, 240 cracks were hence analyzed. The radial crack lengths, from the corners of the indents (see inset in Fig. 1(a)), were measured with an optical microscope and Atomic Force Microscopy (AFM) immediately after indentation. A sketch of the experiment is in Fig. 1(a), and two indentation samples can be seen in Fig. 1(b) and 1(c).

After measuring the length of the cracks (l), the length asymmetry along the polar axis was calculated for each indentation. To verify that the results were not artefacts, we also measured the asymmetry in the direction perpendicular to the polar direction, where in theory there should be none. We define the asymmetry coefficient as

$$\%Asy = \frac{l^+ - l^-}{\langle l \rangle} * 100, \quad (1)$$

where l^+ is the crack length parallel to the polarization, and l^- is the crack length antiparallel to the polarization (up or down in the plan-view photos). For cracks perpendicular to the poling direction, + and – designate right or the left directions, respectively, in the plan-view photos. The average crack length is $\langle l \rangle \equiv \frac{l^+ + l^-}{2}$. Positive (negative) asymmetry indicates a longer (shorter) crack than the average. When cracks have the same length, the asymmetry coefficient is zero.

Figure 2(a) shows the asymmetry of the cracks perpendicular to the polar axis. For these, as expected, there is no asymmetry within statistical error. This lack of perpendicular asymmetry provides a safety check for the robustness of the experimental results. In contrast to the perpendicular cracks, Fig. 2(b) shows that cracks parallel to the poling direction are asymmetric: for P^+ domains, a positive asymmetry is measured, and the asymmetry is reversed for the P^- domains. In other words: crack length parallel to the polarization is always greater than crack length antiparallel to the polarization, irrespective of the polarity of the domain.

The asymmetry of crack length can be used to quantify the asymmetry in fracture toughness, the stress intensity required for creating a crack.^[17] Fracture toughness is given by [18]

$$K_{IC} = 0.016 * \left(\frac{E}{H}\right)^{1/2} \left(\frac{F}{c^{3/2}}\right), \quad H = \frac{F}{2a^2}, \quad (2)$$

where E is the Young Modulus, H the Vickers hardness, F the indent load, c is the distance from the center of the indentation impression to the tip of the crack, and $2a$ is the diagonal of the indent (see inset in Fig.1(a)). Using the values obtained from our tests, K_{IC} was obtained for each crack, and using the expression (1) the asymmetries were calculated.

Figures 2(c) and 2(d) show the asymmetry for the perpendicular and parallel direction, respectively. As explained, there is asymmetry only along the polar axis, i.e. when ferroelectric and flexoelectric polarizations are parallel (crack propagating in the same direction as the ferroelectric polarization), or antiparallel (crack propagating in the opposite direction as the ferroelectric polarization). The average value of the fracture toughness for cracks parallel to the polarization was $\sim 0.24 \pm 0.02 \text{ MPa}\cdot\text{m}^{1/2}$, whereas for the ones antiparallel to the polarization it was $\sim 0.29 \pm 0.03 \text{ MPa}\cdot\text{m}^{1/2}$. In other words, in ferroelectric RKTP, fracture toughness is enhanced (yielding to shorter cracks) by 20% when flexoelectricity and ferroelectricity are antiparallel compared to when they are parallel.

As discussed earlier, since all indentations are performed under the exact same geometrical conditions (same surface, same indenter, same experiment), the asymmetry cannot be a geometrical artifact. The fact that the crack-length asymmetry is reversed for domains of opposite polarization implies that the origin is linked to polarity. Differences in surface adsorbates or near-surface defects can be excluded; even if such differences did exist (and none should be expected given that the polarization is in-plane), each pair of cracks is generated in the same spot and encounters identical surface conditions. The asymmetry in crack propagation is therefore intrinsic and linked to polarity: ferroelectricity acts as a sort of fracture “valve” that can be switched to facilitate or impair crack propagation.

The basis of the asymmetry is the interplay between flexoelectricity and piezoelectricity.^[12-13-19] The local deformation at the tip of the crack generates a flexoelectric polarization that may be parallel or antiparallel to the ferroelectric polarization, resulting in different mechanical response.^[12] For ferroelectrics, there is in theory an additional consideration, which is that the flexoelectric field near the tip of the crack may be large enough to cause local switching of the polarization,^[20-21] thus providing an additional path for energy dissipation that further reduces the available energy for mechanical fracture.

This process, akin to transformation toughening, is known as switching-induced toughening.^[22-24] Switching-induced toughening has so far been studied in ferroelastic-ferroelectrics (i.e. ferroelectric materials where mechanical stress can switch the direction of the polar axis), but flexoelectricity in principle also enables purely ferroelectric (180 degree) switching in non-ferroelastic uniaxial ferroelectrics.^[20] Here we examine the extent to which such effect can contribute to the observed cracking asymmetry of our samples.

Considering a uniaxial ferroelectric, and adding a flexoelectric term to the energy balance, switching should occur when:

$$f_{ijkl}\epsilon_{j,kl}\Delta P_i + E_i\Delta P_i \geq 2P_s E_c \quad (3)$$

where f_{ijkl} is the flexocoupling tensor, $\epsilon_{j,kl}$ is the strain gradient, and ΔP_i are the changes in the spontaneous polarization during the switching, P_s is the magnitude of the spontaneous polarization, and E_c the coercive electric field. Since there is no external electric field, we can discard the second term, and $\Delta P_i = 2P_s$ for 180° domain switching.^[23] The condition for switching thus simplifies to $f_{ijkl}\epsilon_{j,kl} \geq E_c$. In other words, switching happens when the flexoelectric field (left side of the equation) exceeds the coercive field (right side term).

To estimate the size of the switched region, we have considered the longitudinal, transverse, and shear components of the strain gradient, assuming flexocoupling coefficients of the order of $f = 10\text{V}$, as generally observed for ceramics.^[18, 25] With these simplifications, switching should occur in the region of the ferroelectric crystal that satisfies the condition:

$$\left(\frac{\partial \epsilon_{33}}{\partial x_3} + \frac{\partial \epsilon_{11}}{\partial x_3} + \frac{\partial \epsilon_{31}}{\partial x_3} \right) \geq \frac{E_c}{f} \quad (4)$$

Considering the coercive field of RKTP ($E_c = 3.7 \times 10^6 \text{ Vm}^{-1}$)^[26], and with the aforementioned simplifications, a total strain gradient of $\sim 3.7 \times 10^5 \text{ m}^{-1}$ is theoretically required to induce

switching in RKTP. To see whether such strain gradients are reached in the vicinity of the crack, we have used elastic theory to calculate the strain field^[27]

$$\varepsilon_{ij}^{el} = \frac{1+v}{E} \sigma_{ij} - 3 \frac{v}{E} \sigma_m \delta_{ij}, \quad (5)$$

where σ_{ij} is the stress applied to the crack in each direction, and its expression depends on the propagation modes; σ_m is the average stress; E is the Young's Modulus; and v is the Poisson ratio. Focusing on crack mode I (tensile loading), the stress fields in this type of crack are given by the following equations,

$$\sigma_{11} = \frac{K_I}{\sqrt{2\pi r}} \cos \frac{\theta}{2} \left(1 - \sin \frac{\theta}{2} \sin \frac{3\theta}{2} \right) \quad (6)$$

$$\sigma_{22} = \frac{K_I}{\sqrt{2\pi r}} \cos \frac{\theta}{2} \left(1 + \sin \frac{\theta}{2} \sin \frac{3\theta}{2} \right) \quad (7)$$

$$\tau_{12} = \frac{K_I}{\sqrt{2\pi r}} \cos \frac{\theta}{2} \sin \frac{\theta}{2} \cos \frac{3\theta}{2}, \quad (8)$$

where K_I is the intensity factor (fracture toughness for this calculation). Transforming equations (6), (7) and (8) to Cartesian coordinates and using Mathematica^[28] for the calculations, we have computed analytically the strain field in equation (5), and the strain gradient associated with it. The value used for the intensity factor (fracture toughness) was the one obtained in this study, $K_I = 0.29 \text{ MPa} \cdot \text{m}^{1/2}$; all other values were taken from the literature.^[29]

The calculated flexoelectric field map around a crack tip in RKTP is plotted in Fig. 3(a). The dashed line outlines the region within which flexoelectricity is large enough to induce local switching of the polarization. The calculated size of this switching region (~20nm), however, is very small. It is at the edge of thermodynamic stability of a switched domain embedded in a non-switched matrix,^[21, 30-31] so switch-back is almost certain to happen, plus the domain size is also close to the resolution limit of Piezoresponse Force

Microscopy (PFM). We examined the cracks by PFM finding no evidence of 180° local switching near them.

In order to look for evidence of crack-induced flexoelectric switching, we turn to another uniaxial ferroelectric, Lithium Niobate (LN). Since flexoelectricity is proportional to dielectric permittivity,^[32] it is to be expected that the higher dielectric constant of LN ($\epsilon_r(LN) = 37$; $\epsilon_r(KTP) = 13$),^[33] the local flexoelectric switching may be enhanced. Using the coercive field for LN $E_c = 2.1 \times 10^7 \text{ V m}^{-1}$,^[34] and its flexocoupling coefficient,^[13] the strain gradient required to induce local switching is $4.2 \times 10^5 \text{ m}^{-1}$. Using equations (5) – (8), and the elasticity values in the literature,^[35 -36] we mapped the flexoelectric field (Fig. 3(b)) and found that the switching radius is $\sim 40 \text{ nm}$ around the tip, which is theoretically big enough to be stable and detectable at room temperature. This prediction was experimentally tested in a crystal of LN, y-cut, indented in the same conditions as with the RKTP sample.

The Lateral Piezoresponse Force Microscopy (LPFM) images of the resulting indent and cracks are shown in Fig. 4. In LN, the easy fracture plane is at 60 degrees with respect to the polar axis, and the cracks tend to zig-zag instead of following a clean straight line along the polar axis. Although this makes it impossible to reliably measure and compare their lengths, it does not affect their ability to generate flexoelectric fields. Indeed, the PFM images in Fig. 4(b) and 4(c) show that cracks with a propagation component antiparallel to the polarization induce local 180 degree switching, leaving a trail of needle domains in the crack's wake. This "flexoelectric switching" is analogous to the mechanical writing of ferroelectric domains using Atomic Force Microscopy (AFM) tip indentation.^[20] The mechanical consequences, however, are profound: since switching dissipates energy, the cracks that switch polarization dissipate more energy and thus cannot grow as long as those that do not. Consequently, fracture patterns in ferroelectrics must necessarily be asymmetric.

In summary, the interaction between flexoelectricity and ferroelectricity in fracture fronts leads to qualitatively new phenomena. First, the observation that crack-induced flexoelectricity can cause ferroelectric switching shows that crack propagation can modify polarity. Second, and conversely, polarity affects crack propagation, making it asymmetric. These findings have practical implications, as they suggest that fatigue due to microcracking could be mitigated or enhanced according to the poling direction of the ferroelectric. Finally, crack-diode-like functionality offers a new degree of freedom for crack-based nanopatterning.^[3] The discovery also implies that the assumption of mechanical inversion symmetry is fundamentally wrong for situations involving inhomogeneous deformation of piezoelectric materials. The results demonstrate that flexoelectricity has to be taken into account in any realistic model of fracture in such materials.

Acknowledgements

The authors thank Dr. Neus Domingo for valuable discussions. K.C.-E. and G.C. acknowledge ERC Starting Grant 308023. ICN2 is supported by the Severo Ochoa program from Spanish MINECO (Grant No. SEV-2013-0295), and also funded by the CERCA Programme / Generalitat de Catalunya. H.K. and C.C. acknowledge the Swedish Research Council for generous support. J.S work has been partially funded by the 2017-SGR-292 project from the Generalitat de Catalunya and the MAT2017-86357-C3-1-R project from the Spanish Ministerio de Economía y Competitividad (MINECO), cofinanced by the ‘Fondo Europeo de Desarrollo Regional (FEDER).

References

1. Broek, D. *Elementary Engineering Fracture Mechanics*. Martinus Nijhoff Publishers, 4th edn (1986).
2. D. Francois, A. Pineau, and A. Zaoui, *Mechanical Behaviour of Materials*. Springer press, 2nd ed. (2012).
3. K. H. Nam, I. H. Park & S. H. Ko. *Nature* **485**, 221–224 (2012).
4. S. Kim & Q. Jiang. *Smart Mater. Struct.* **5** 321 (1996).
5. J. Shieh, J. E. Huber & N.A. Fleck. *J. Eur. Ceram. Soc.* **26**, 95 – 109 (2006).
6. S. Kogan. *Sov. Phys. Solid State* **5**, 2069-2079 (1964).
7. E. Cross. *J. Mater Sci.* **41**, 53-63 (2006).
8. P. Zubko, G. Catalan & A.K. Tagantsev. *Annu. Rev. Mater. Res.* **43**, 387 – 421 (2013).
9. M. Gharbi, Z.H. Sun, P. Sharma & K. White. *Appl. Phys. Lett.* **95**, 142901 (2009).
10. C.R. Robinson, K.W. White & P. Sharma. *Appl. Phys. Lett* **101**, 122901 (2012).
11. H. Zhou, Y. Pei, F. Li, H. Luo & D. Fang. *Appl. Phys. Lett* **104**, 061904 (2014).
12. A. Abdollahi, C. Peco, D. Millán, M. Arroyo, G. Catalan & I. Arias. *Phys. Rev. B* **92**, 094101 (2015).
13. K. Cordero-Edwards, N. Domingo, A. Abdollahi, J. Sort & G. Catalan. *Adv. Mater.* **29**, 1702210 (2017).
14. F. Vásquez-Sancho, A. Abdollahi, D. Damjanovic & G. Catalan. *Adv. Mater.* **30**, 1705316 (2018)
15. A. Zukauskas, V. Pasiskevicius & C. Canalias. *Opt. Express* **21**, 1395 (2013).
16. C. Liljestrand, A. Zukauskas, V. Pasiskevicius & C. Canalias. *Opt. Lett.* **42**, 2435-2438 (2017).
17. A.C. Fischer – Cripps. *Introduction to contact mechanics*. Springer press, 2nd ed. (2007).
18. G.R. Anstis, P. Chantikil, B.R. Lawn & D.B. Marshall, *J. Amer. Ceram. Soc.* **62**, 347-359 (1979).
19. Zhou, H., Pei, Y., Li, F., Luo, H. & Fang, D. *Appl. Phys. Lett.* **104**, 061904 (2014).
20. H. Lu, C. –W. Bark, D. Esque de los Ojos, J. Alcalá, C. B. Eom, G. Catalán & A. Gruverman. *Science* **336**, 59 (2012).
21. J. Ocenásek, H. Lu, C. W. Bark, C. B. Eom, J. Alcalá, G. Catalan & A. Gruverman, *Phys. Rev. B* **92**, 035417 (2015).
22. S.C. Hwang, C.S. Lynch & R.M. McMeeking. *Acta Metall. Mater.* **43**: 2073 – 2084 (1995).
23. X. Zeng & R.K.N.D Rajapakse. *Smart Mater. Struct* **10**, 203 – 211 (2001).
24. G.A. Schneider. *Annu. Rev. Mater. Res.* **37**, 491 – 538 (2007).

25. J. Narvaez, S. Saremi, J. Hong, M. Stengel & G. Catalan. *Phys. Rev. Lett.* **115**, 037601 (2015).
26. A. Zukauskas, G. Strömqvist, V. Pasiskevicius, F. Laurell, M. Fokine, and C. Canalias. *Opt. Mater. Express* **1**, 1319-1325 (2011).
27. B. Lawn, *Fracture of brittle solids*. Cambridge University Press, 2nd ed. (1993).
28. W. R. Inc., *Mathematica, Version 10.2*, champaign, IL, 2016.
29. S. Haussuhls, S. Luping, W. Baolin, W. Jiyang, J. Liebertz, A. Wostracke & Ch. Fink. *Cryst. Res. Technol.* **29**, 4 (1994).
30. J. Y. Jo, D. J. Kim, Y. S. Kim, S.-B. Choe, T. K. Song, J.-G. Yoon, & T. W. Noh. *Phys. Rev. Lett.* **97**, 247602 (2006).
31. J. Y. Jo, Y. S. Kim, T. W. Noh, J.-G. Yoon, & T. K. Song. *Appl. Phys. Lett.* **89**, 232909 (2006).
32. A. K. Tagantsev. *Phys. Rev. B* **34**, 5883 (1986).
33. J.D. Bierlein & H. Vanherzeele. *J. Opt. Soc. Am. B* **6**, 622 (1989).
34. V. Gopalan, V. Dierolf & D.A. Scrymgeour. *Annu. Rev. Mater.* **37**, 449–489 (2007).
35. A.W. Warner, M. Onoe, & G.A. Coquin, *J. Acoust. Soc. Am.* **42**, 1223 (1967).
36. R.T. Smith & F.S. Welsh, *J. Appl. Phys.* **42**(6), 2219 (1971).

Figure 1: (a) Schematic of the Vickers Indentation test showing the top view of typical radial crack propagation for indentation fracture toughness measurement with corresponding crack (l) and diagonal lengths ($2a$). AFM topography of Vickers indent in RKTP showing the radial crack propagation for (b) up ($l_{\parallel}^+ = 10.85 \mu m$; $l_{\perp}^+ = 9.87 \mu m$; $l_{\parallel}^- = 8.53 \mu m$; $l_{\perp}^- = 10.51 \mu m$) and (c) down ($l_{\parallel}^+ = 8.88 \mu m$; $l_{\perp}^+ = 11.04 \mu m$; $l_{\parallel}^- = 10.74 \mu m$; $l_{\perp}^- = 11.35 \mu m$) polarization.

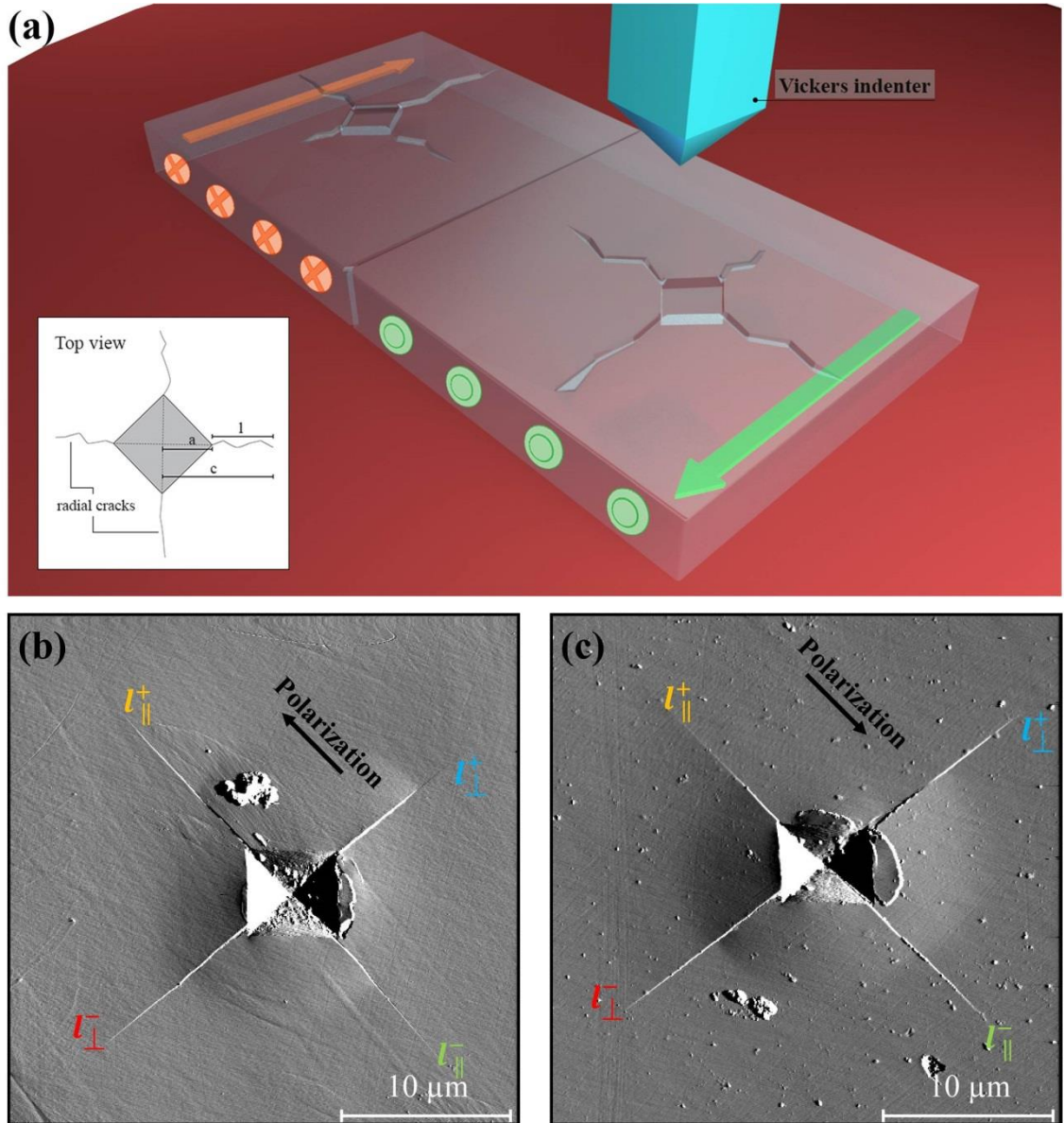


Figure 2: Crack length asymmetry (a) perpendicular and (b) parallel to the polar axis.

Fracture toughness asymmetry (c) perpendicular and (d) parallel to the polar axis.

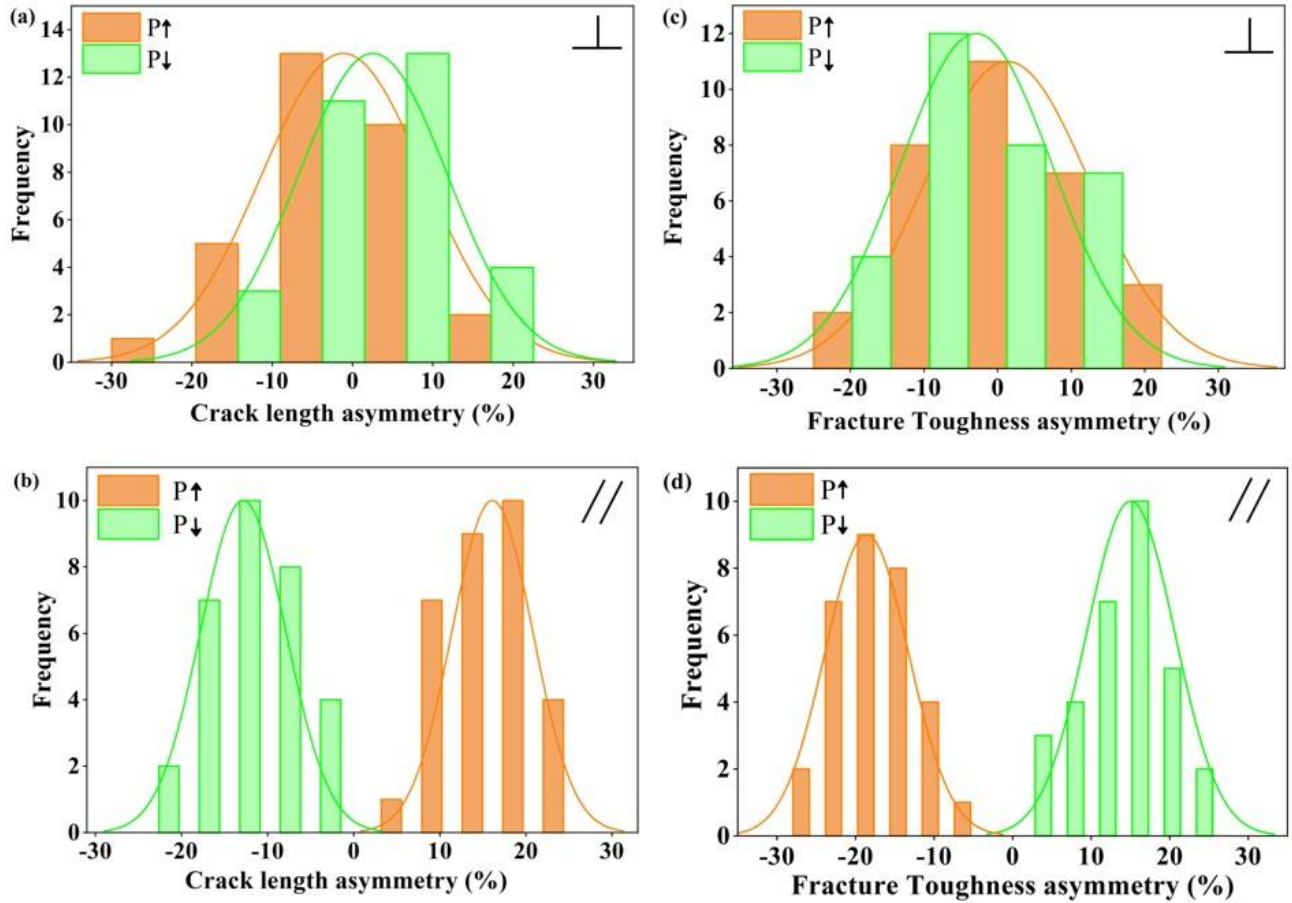


Figure 3: Calculated distribution of the flexoelectric field around the apex of a crack in (a) RKTP, and (b) in LN. The black line marks the region where the gradient-induced electric field is strong enough to be able to induce local switching of the polarization.

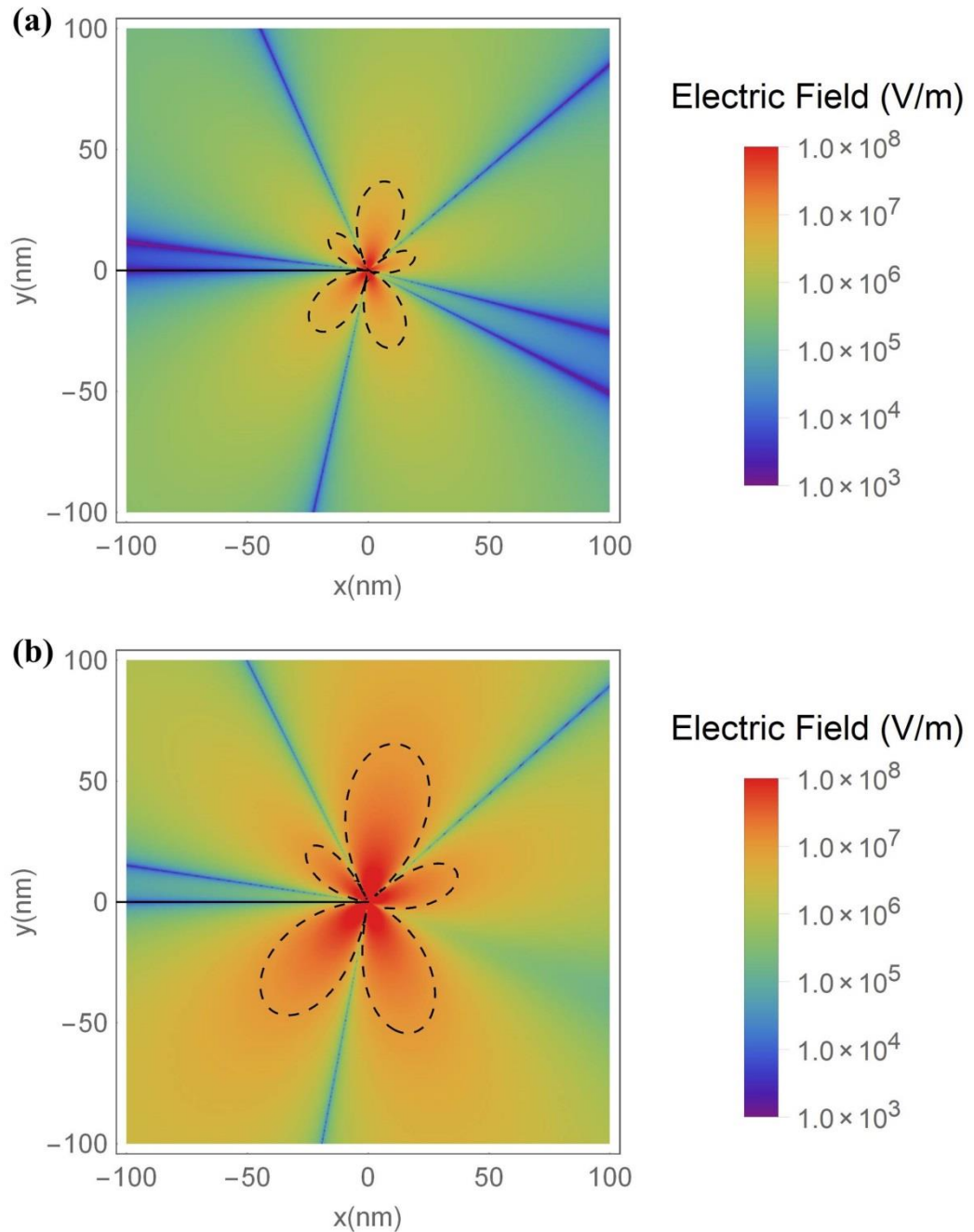


Figure 4: (Center) AFM topography of Vickers indent in LN y-cut showing the radial crack propagation. LPFM amplitude and phase of crack propagating parallel (left) and antiparallel (right) showing local switching as the crack propagates opposite to the polarization of the crystal.

